CHEMBIOCHEM

DOI: 10.1002/cbic.200800329

Resin-Bound Aminofluorescein for C-Terminal Labeling of Peptides: High-Affinity Polarization Probes Binding to Polyproline-Specific GYF Domains

Viviane Uryga-Polowy,[a, b] Daniela Kosslick,[b, c] Christian Freund,[b, c] and Jörg Rademann*[a, b]

A polymer support for the solid-phase synthesis of C-terminally labeled carboxylic acids has been developed. Fluorophore-labeled peptides were constructed directly on the amino group of resin-bound aminofluorescein. Fmoc-protected aminofluorescein was coupled onto tritylpolystyrene, and the free phenolic hydroxyl positions of the fluorescein were blocked with suitable protecting groups. The mode of attachment was analyzed and found to be selective for the phenoxy ether linkage. The conditions for peptide synthesis on the labeling resin were investigated, and a small library of C-terminally labeled peptides was prepared. The fluorescence quantum yields of C-terminally labeled peptides were determined and indicated the suitability of the compounds for imaging and binding experiments. The obtained peptides were therefore investigated as fluorescence polarization probes. Two different proline-rich binding domains of the GYF family—CD2BP2 and PERQ2—were targeted by peptides labeled either C- or N-terminally. Reversible binding constants were determined by fluorescence polarization measurements and were verified by competition experiments with the corresponding unlabeled peptide. As a second control, the binding constants were measured by NMR titration experiments, recording the HSQC NMR spectra of ^{15}N-labeled proteins in the presence of the peptide polarization probes. Ligands with higher affinities than all others known previously were identified for both GYF domains. The competition assay with the developed fluorescent probe has a high statistical reliability and can thus be used for screening of GYF domain inhibitors.

Introduction

Fluorescence-labeled molecules are essential tools in biochemical and biomedical research. Attached fluorophores allow labeled molecules in cells and organisms to be traced by fluorescence microscopy or fluorescence lifetime imaging (FLIM),[1] fluorescence-assisted cell sorting (FACS),[2] and NIR imaging.[3] In addition, fluorophore-labeled molecules can provide information relating to specific intermolecular interactions both in vitro and in living cells, diffusion rates, and molecular dynamics through fluorescence resonance energy transfer (FRET)[4] and fluorescence correlation spectroscopy (FCS).[5] One method widely used for the detection and quantification of binding phenomena is fluorescence polarization (FP).[6]

We were interested in developing fluorescence-based methods for the characterization of protein–protein interactions and the identification of small-molecule inhibitors through high-throughput screening (HTS) of chemical libraries. Specific peptide and small-molecule inhibitors of protein–protein interactions can be valuable tools for studying the functional significance of single interactions and hence elucidation of their roles in complex networks governing cellular functions. Moreover, if pharmacologically relevant protein–protein interactions are studied, the identified inhibitors may serve as starting points for drug development.

We were interested specifically in GYF domains as protein targets, since they represent a prototypic class of protein interaction domains.[7] Like SH3 and WW domains they recognize proline-rich sequences and thereby contribute to the organization of cellular signaling by forming protein-interaction networks. Two GYF domains (CD2BP and PERQ2) were selected as targets. CD2BP GYF is involved in lymphoid signal transduction[7] and, supposedly, in the spliceosome.[8] For both domains, binding peptides of moderate affinity have been identified by phage display technology.[9]

Fluorescence polarization (FP) was selected as method of choice for our bioassay development for several reasons. Many protein–protein interactions can be reduced to protein–peptide interactions. A fluorescence-labeled derivative of an optimized peptide ligand can therefore be used as a probe for small-molecule inhibitor screens by using FP competition experiments. FP assays can be operated in homogeneous solution, thereby eliminating the surface and multivalency effects that hamper heterogeneous assays such as enzyme-linked formats (e.g., ELISA) and those based on plasmon resonance

[a] *V. Uryga-Polowy, Prof. Dr. J. Rademann*
Department of Medicinal Chemistry
Leibniz Institute for Molecular Pharmacology (FMP)
Robert-Rössle-Strasse 10, 13125 Berlin (Germany)
Fax: (+49) 30-94062901
E-mail: rademann@fmp-berlin.de

[b] *V. Uryga-Polowy, D. Kosslick, Dr. C. Freund, Prof. Dr. J. Rademann*
Institute for Chemistry and Biochemistry, Free University Berlin
Takustrasse 3, 14195 Berlin (Germany)

[c] *D. Kosslick, Dr. C. Freund*
Protein Engineering Group
Leibniz-Institute for Molecular Pharmacology (FMP)
Robert-Rössle-Strasse 10, 13125 Berlin (Germany)

(e.g., BIACore). Furthermore, they enable high-throughput measurements with low protein consumption.

The development of a novel FP assay requires an appropriate selection of fluorophore and protein construct, with fluorescence lifetime and molecular weight characteristics that make it possible to distinguish between the free and bound states of the fluorescent ligand. The method is based on the direct observation of the rotational correlation time (θ) of the fluorescent molecule under investigation relative to the fluorescence lifetime (τ) of the excited fluorophore.[10] In the case that the molecule tumbles slowly ($\theta_{moiety} \gg \tau_{fluorophore}$), the anisotropy (polarization) of the fluorescence excitation light is retained in the emission light (Figure 1). Since θ is a function of the molecular weight,[11] depolarization takes place rapidly for a small molecule with low molecular weight and small specific volume, whereas the same labeled molecule bound to a macromolecule—a protein, for example—will emit strongly polarized light.

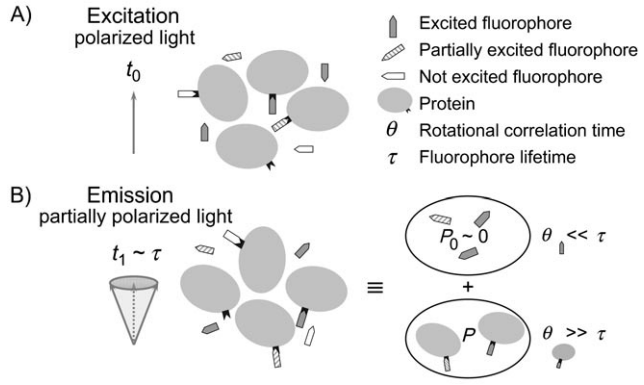

Figure 1. Principle of fluorescence polarization assays. A) All fluorophores aligned with the polarization plane are excited. B) Free fluorophores rotate rapidly and the emitted light is no longer polarized. Fluorophores bound to large molecules rotate more slowly, and the polarization is mostly retained in the emitted light.

The synthesis of a suitably labeled fluorescence probe in praxi is essentially the result of an extended optimization process.[12] A fluorophore attached to the ligand distant from the binding site might retain its mobility to a large degree, resulting in a significant reduction of the polarization signal. The very same fluorophore attached too closely can interfere with ligand binding, reducing affinity and increasing the K_D value. An optimal FP probe possesses high affinity together with a maximum signal-to-noise ratio and a high statistical reproducibility of the recorded polarization data, resulting in an assay characterized by a high Z' value.[13]

Conventional approaches for fluorophore labeling of peptides and proteins employ readily available compounds such as fluorescein 5(6)-isothiocyanate (FITC), 5(6)-carboxyfluorescein, 5(6)-tetramethylrhodamine isothiocyanate (TRITC), or 2-dimethylaminonaphthalene-5(6)-sulfonyl chloride (dansyl chloride). All these fluorophores are coupled to nucleophilic sites of the protein, such as the amino groups of lysine residues[14] or the N termini of peptides.[15]

We needed an inexpensive, robust, and efficient fluorophore attachment method. The protocol should allow the labeling of diverse sets of molecules with fluorophores and should avoid additional workup procedures in the preparation of labeled libraries. To reduce the conformational flexibility, it was necessary to avoid spacers for fluorophore attachment. From this list of specifications we concluded that a reactive fluorophore directly attached to a polymer support should fulfill the requirements best.

Results and Discussion

Selection of the fluorophore

Fluoresceinamine was selected for the development of a labeling resin. Acylated fluoresceinamine possesses a long emission wavelength ($\lambda_{exc} = 492$ nm; $\lambda_{em} = 519$ nm) well-suited for library screening because it does not interfere with the intrinsic fluorescence of most small molecules and proteins, thus reducing the number of potential false positives. The short fluorescence lifetime (4.5 ns[16]) and the good quantum yield of fluorescence enable sensitive discrimination of binding events between labeled low molecular weight compounds and larger proteins as predicted by the Perrin equation.[17,18] After we had investigated the synthesis of fluorophore libraries in solution by various protocols (V. Uryga-Polowy, unpublished results), a solid-phase approach[19] appeared to be superior to synthesis in solution. Reagents and byproducts can easily be removed by washing steps, and completion of reactions can be achieved by adding reagents in excess or by repeating the reaction steps, enabling isolation of pure products without chromatographic purification. A labeling reagent on solid support can also be used as a starting point for further already established syntheses on solid phase, such as solid-phase peptide synthesis (SPPS).[20]

Synthesis of the fluorescein labeling resin

2-Chlorotrityl chloride resin was selected for attaching the fluorophore building block. Direct coupling of unprotected 4-aminofluorescein (**1**, Scheme 1) to the 2-chlorotrityl chloride resin in the presence of DIPEA led only to alkylation of the aniline nitrogen. As a control, the analogous reaction between trityl chloride and 4-aminofluorescein was conducted in solution, and NMR analysis confirmed the selective formation of the *N*-tritylated product. Thus, for controlled coupling to the polymer support, the aniline moiety was protected with the 9-fluorenylmethoxycarbonyl (Fmoc) group, yielding carbamate **4**. The Fmoc protecting group, being labile under basic conditions, is orthogonal to the resin cleavage conditions and allows direct evaluation of the resin loading by photometric quantification of cleaved Fmoc groups.[20]

Building block **4** was obtained by two alternative strategies. Direct carbamoylation of **1** furnished **4** in a single step in 40% yield after flash chromatography. The major by-product of this reaction, doubly protected aminofluorescein, could be recovered by chromatography and recycled as starting material. Alternatively, **4** was prepared in three steps via the pivaloyl-pro-

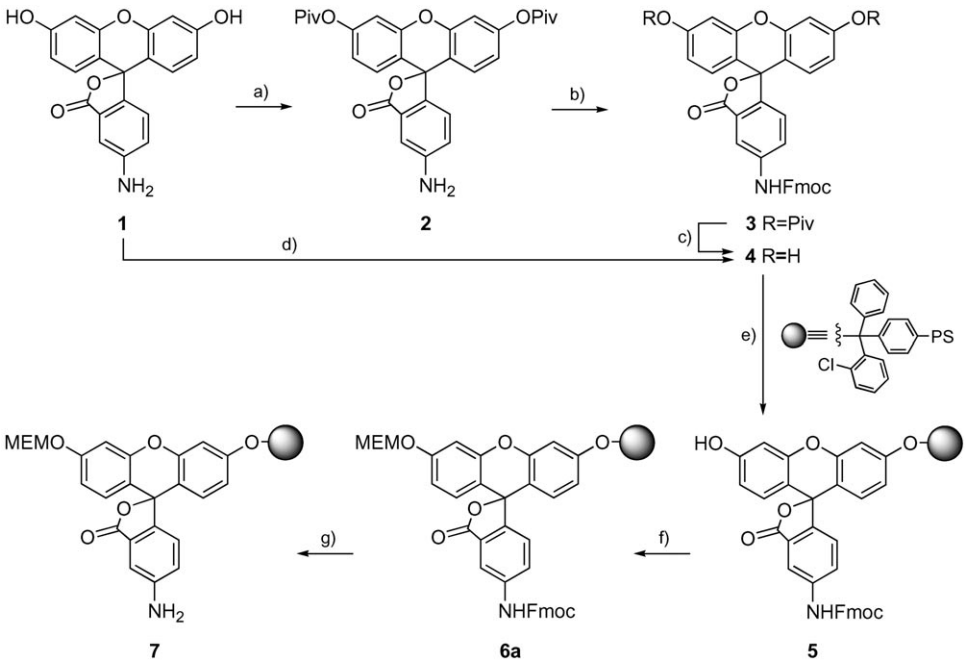

Scheme 1. Synthesis of the fluorescein labeling resin. Conditions: a) Piv_2O, Cs_2CO_3, DMF, RT, 90 min, 96%; b) Fmoc-Cl, NaOH, THF, 0 °C→RT, 16 h, 84%; c) 95% TFA in H_2O, 60 °C, 120 min, 92%; d) Fmoc-Cl, NaOH, THF, 0 °C→RT, 16 h, 40%; e) 2-chlorotrityl chloride resin, DIPEA, DCM/DMF, RT, 180 min; f) MEM-Cl, DIPEA, DMF, RT, 90 min; g) 20% piperidine in DMF, RT, 2 min+10 min.

tected intermediate **2** (Scheme 1)[21] in a procedure that worked smoothly and required only the intermediate crystallization of **3** to furnish **4** in an overall yield of 72%, avoiding purification by chromatography.

Coupling of **4** to 2-chlorotrityl resin by treatment with DIPEA in DCM/DMF succeeded in providing **5** with a practical loading of 0.35 mmol g^{-1}. The yield of 45% could not be increased either by heating or by use of excess reagent; presumably the maximum loading of the resin is limited by partial cross-coupling.

The mode of attachment was next investigated. Depending on the pH value, fluorescein can exist as four prototropic species[22,23]—as a cation, a neutral species, a monoanion, or a dianion—and so, with allowance for all tautomers, seven different structures can be formed (Scheme 2A). The monoanion is found predominantly (99.9%) as the carboxylate **9a**, with a pK_a value of 6.4. Thus, under the basic conditions applied here, the dianion **12** possessing a carboxylate and a phenoxide nucleophile is formed, furnishing either the trityl ester product **13** or the trityl ether product **14** (Scheme 2B). Although phenoxides are in general better nucleophiles than carboxylates, in this case their reactivity might be impaired by delocalization of the negative charge or by steric effects, so the selectivity of the alkylation step had to be verified experimentally. The ATR-IR (attenuated total reflection IR) spectrum of resin **5** after Fmoc removal displayed an absorption band at 1762 cm^{-1} characteristic of a lactone carbonyl vibration (Figure 2) indicating selectivity for the trityl ether product **14**. The ester or carboxylate carbonyl groups would resonate at significantly lower wave numbers (1730–1710 cm^{-1} or <1700 cm^{-1}, respectively).[24]

This analytical finding was supported by further experimental evidence. The mono-*O*-pivaloyl-protected derivative of **4** was isolated and coupled to trityl resin, resulting in a poor yield (10%) of immobilized fluorescein. In this case, dianion formation was excluded due to the protection of one phenolic position, and only the monoanion with the equilibrium on the side of the less reactive carboxylate was available for alkylation, resulting in the observed low coupling yield.

The immobilized fluorescein **5** still had two potentially reactive sites. In order to ensure selective reactions of the aniline moiety, the free phenol had to be protected. The selected protecting group should be removable under acidic conditions together with final cleavage of products of the resin, and should be eliminated from the solution by evaporation. 2-Methoxyethoxymethyl (MEM), *tert*-butyldimethyl silyl (TBDMS), and triethylsilyl (TES) ethers were investigated for this purpose, yielding resins **6a**, **6b**, and **6c**, respectively (Scheme 3). The efficient use of these three groups was evaluated by LC/MS analysis of the product cleaved from the resin after Fmoc removal and treatment with Fmoc-glycine. All three groups provided product **15** with high purity in excellent yields. The silyl ethers, however, were slightly labile on base treatment, whereas the MEM group was totally stable under these conditions and was therefore selected as the best choice for the subsequent syntheses.

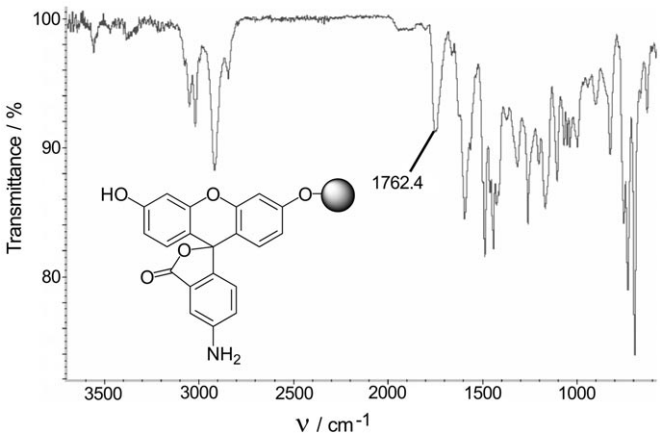

Figure 2. ATR-IR spectrum of the resin resulting from Fmoc deprotection of resin **5**. The characteristic C=O band at 1762 cm^{-1} shows the presence of a lactone ring and not an ester, confirming the fluorescein attachment to the resin on the phenol.

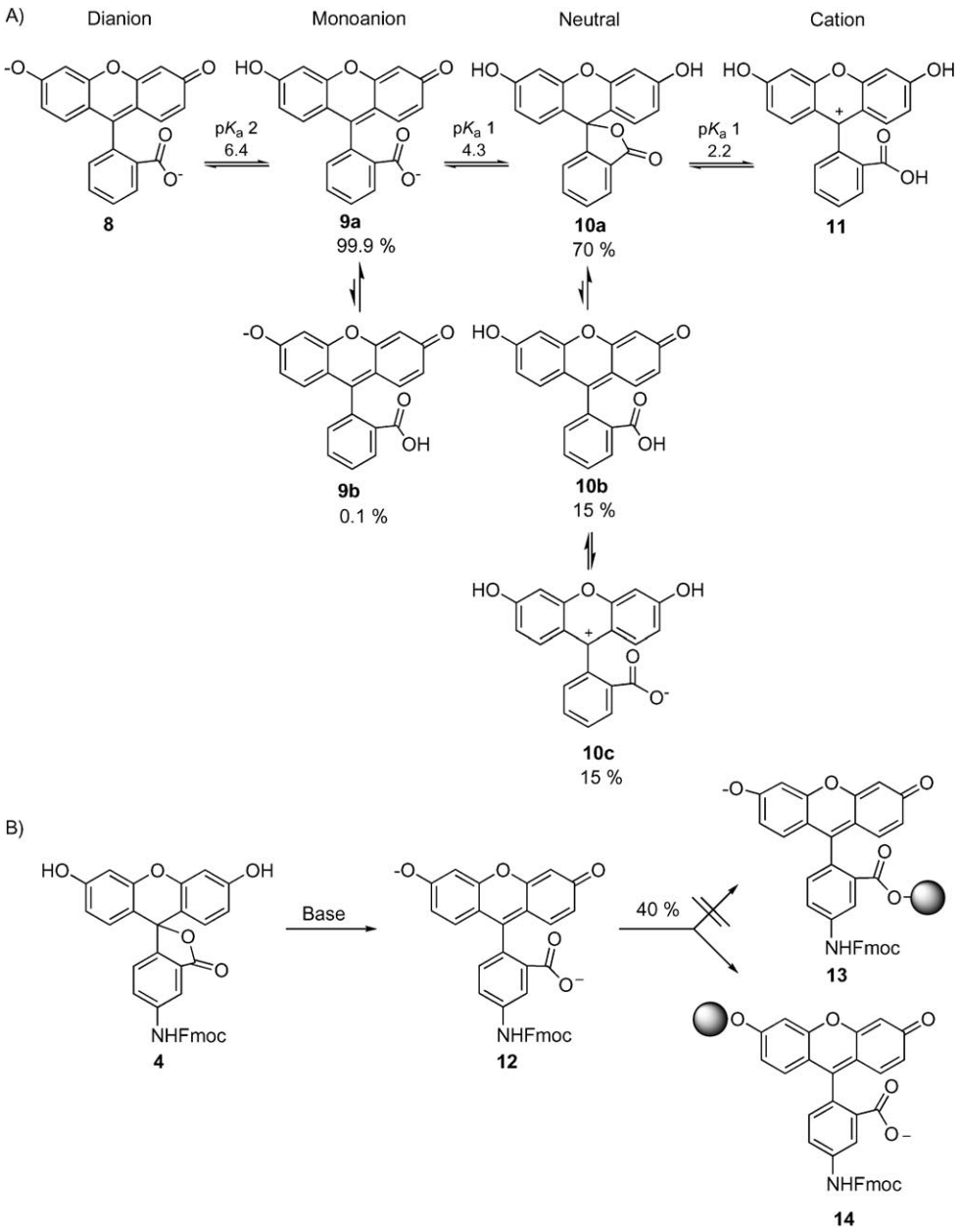

Scheme 2. A) The prototropic forms of fluorescein. B) Attachment mode to the trityl resin.

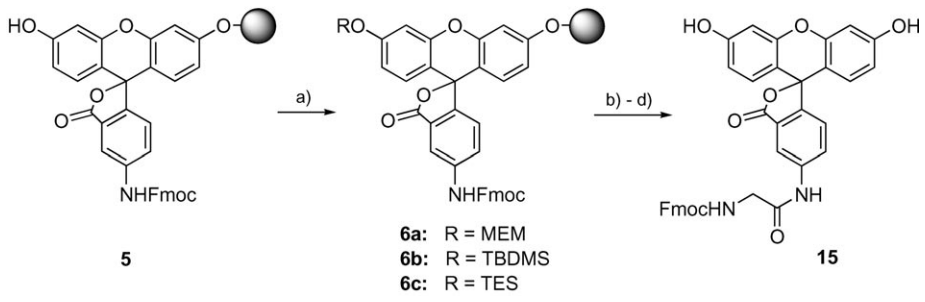

Scheme 3. Phenol protection. Conditions: a) i: MEM-Cl, DIPEA, DMF, RT, 2×2 h; ii: TBDMS-Cl, DIPEA, DMF, RT, 2×2 h; iii: TES-Cl, DIPEA, DMF, RT, 2×2 h; b) 20% piperidine in DMF, RT, 2×15 min; c) Fmoc-AA, DIC, THF/DCM, RT, 60 min; d) 95% TFA/H_2O.

Synthesis of a library of C-terminally fluorescein-labeled peptides

After the protection of resin **5** to yield **6a**, the Fmoc group was removed, and acylation of the aniline **7** with Fmoc-protected amino acids was investigated. Different conditions were tested (Table 1),[25–27] and coupling with diisopropylcarbodiimide in DCM/THF (Table 1, entry 6) showed the best results for formation of cleavage product **15** (92%). After the Fmoc group had been removed, peptide synthesis (Scheme 4) was conducted with amine **16** by the Fmoc strategy, with alternating DIC/HOBt coupling steps and piperidine Fmoc removal. Finally, the peptidyl-aminofluorescein resins **17** were N-terminally acylated (**18**) and cleaved from the resin with 95% TFA/H_2O and 2% triisopropylsilane to yield peptides **19**. Phenol was added as a scavenger in the cases of peptides containing the Pmc protecting group.

The fluorescence properties of the obtained C-terminally labeled peptides were investigated and compared to those of well-known N-terminally labeled peptides. Whereas 5(6)-carboxyfluorescein is highly fluorescent on its own,[28] 4-aminofluorescein is practically nonfluorescent in its amine form. On functionalization, the fluorescence properties of both molecules are changed and these variations were investigated by measurement of fluorescence emission spectra (Figure 3). Amidation of 5(6)-carboxyfluorescein (peptide **19l**) leads to a reduction in the fluorescence quantum yield to 0.44, whereas acylation of 4-aminofluorescein (peptide **20a**) causes a drastic increase in fluorescence (Table 2). As a result, the novel C-terminally labeled and the classical N-terminally labeled peptides have similar exci-

Table 1. Coupling conditions on the fluorescein resin.

	Amino acid (5 equiv)	Activating agent (5 equiv)	Base (5 equiv)	Solvent	Conversion [%]
1	Fmoc-Gly-OH	DIC/HOBt	–	DMF	0
2	Fmoc-Gly-OH	DIC	–	DMF	0
3	Fmoc-Gly-OH	DIC	–	THF	9
4	Fmoc-Gly-OH	DIC	–	DCM	77
5	Fmoc-Gly-OH	DIC/HOBt	–	DCM	68
6	Fmoc-Gly-OH	DIC	–	THF/DCM (1:1)	92
7	Fmoc-Gly-OH	HATU	DIPEA	DMF	92
8	Fmoc-Gly-OH	HATU	DIPEA	DCM	91
9	Fmoc-Gly-OH	HATU	collidine	DMF	77
10	Fmoc-Gly-OH	HATU	collidine	DCM	73
11	Fmoc-Gly-OH	HATU	2,6-lutidine	DMF	60
12	Fmoc-Gly-OH	HATU	2,6-lutidine	DCM	50
13	FmocNH-CH_2-COF	–	DIPEA	DCM	78

Conditions: a) Amino acid, activating agent, base, solvent, 90 min, 25 °C; b) 20% piperidine in DMF, RT, 2× 15 min.

tation and emission maxima and fluorescence quantum yields.

The newly established methodology for the synthesis of C-terminally labeled fluorescein peptides was subsequently applied for the development of fluorescence probes for two protein interaction domains that bind to proline-rich sequences (PRSs). The GYF domain of the CD2-binding protein (CD2BP2) is involved in mediating molecular interactions within the spliceosome, while the functional role of the PERQ2 GYF domain is largely unknown. However, peptide binding specificities for both domains have been characterized,[9,29] and phage display had previously identified peptides with binding affinities below 100 μM, a typical value for proline-rich sequence recognition domains. All GYF domain binding peptides converge on a central PPG core motif, while residues directly flanking this sequence vary between the individual GYF domains investigated so far. For the GYF domain of CD2BP2, the peptide EFGPPPGWLGR derived from phage display[9] was used as a starting point for the probe development, while for PERQ2 we started from the peptides FNGSPPGLSRD and WRPGPPPPPPPGLV. For each domain, a focused library of fluorescent probes was synthesized, with positioning of the fluorophore either C-terminally (Table 3, **19a**–**m**, 13 peptides) or N-terminally (Table 4, **20a**–**s**, 19 peptides). Both the peptide length and the nature of amino acids were varied systematically for K_D optimization.

Fluorescence polarization assays

For fluorescence polarization measurements, peptides were dissolved in DMSO at 10 mM and diluted in PBS buffer (pH 7.3). In the final assay mixture, the concentration of the fluorescent peptide was maintained constant at 10 nM, and increasing amounts of protein were added over a concentration range of 0.01 μM to 350 μM. Although no aggregation was observed, Tween 20 (0.1%) was used in all assays as a detergent. To reduce the already low protein consumption of FP experiments to a minimum, the assay was performed with very good reproducibility in round-bottomed, very low-volume microtiterplates at a final assay volume of 6 μL. After addition of protein

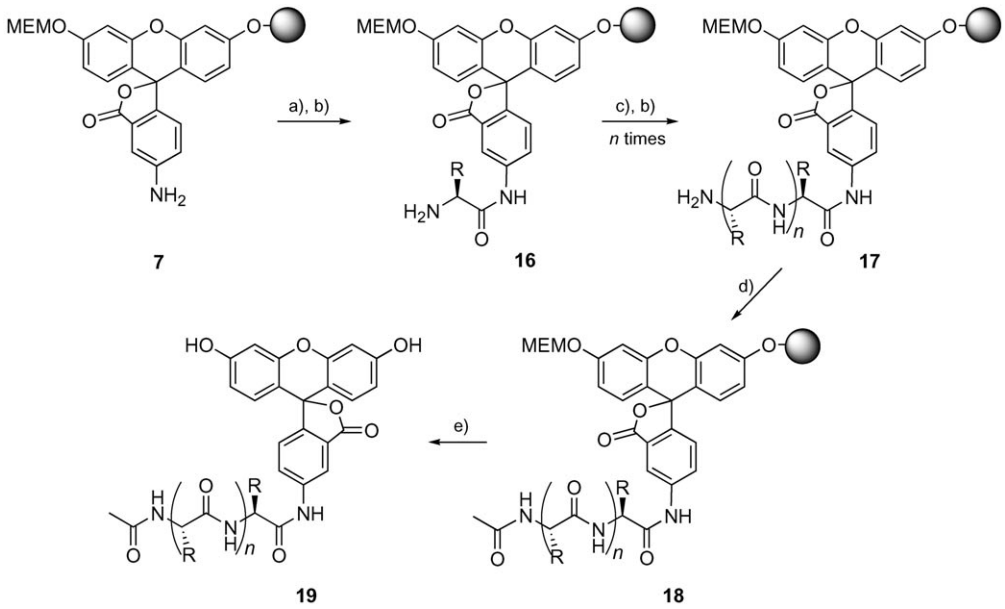

Scheme 4. Solid-phase synthesis of C-terminally fluorescein-labeled peptides. Conditions: a) Fmoc-AA, DIC, THF/DCM, RT, 60 min; b) 20% piperidine in DMF, RT, 2×15 min; c) Fmoc-AA, DIC, HOBt, DMF, 30 min; d) Ac_2O, DIPEA, DMF, RT, 15 min; e) 95% TFA in H_2O, PhOH (if Pmc protecting group), TMS (if Trt protecting group).

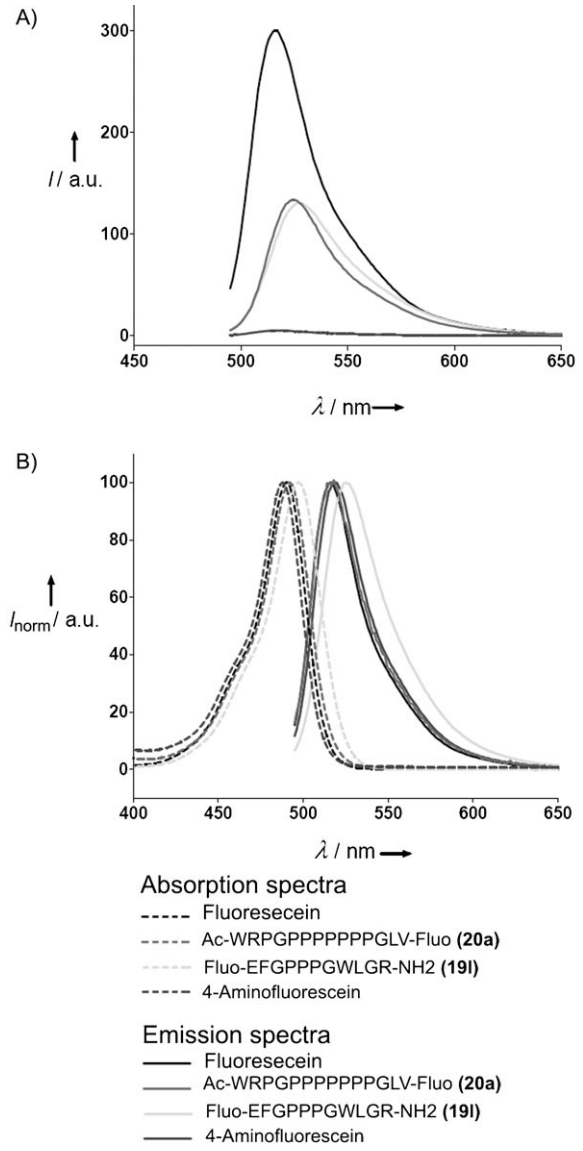

Figure 3. A) Fluorescence emission spectra of the C- and N-terminally labeled peptides **20a** and **19l**, 4-aminofluorescein, and fluorescein. B) Normalized absorption and emission spectra. The acetylated 4-aminofluorescein present in **20a** delivers a signal intensity similar to that of the 5(6)-carboxyfluorescein present in **19l**, whereas non-acetylated 4-aminofluorescein is almost nonfluorescent. Furthermore, the absorption and emission wavelengths of the C-terminally labeled peptide **20a** are more similar to those of fluorescein than those of the N-terminally labeled **19l**.

Table 2. Fluorescence quantum yields (ϕ_{fl}) and absorption and emission maxima (λ_{abs}, λ_{em}) of C- and N-terminally fluorescein labeled peptides in NaOH (0.1 M), determined by comparison with a fluorescein standard solution.

Compound	ϕ_{fl}	λ_{abs} [nm]	λ_{em} [nm]
19l	0.49	497	525
20a	0.44	492	519
4-aminofluorescein	0.02	488	518
fluorescein	0.95	490	516

Table 3. Synthesized C-terminally fluorescein-labeled peptides for CD2BP2 and PERQ2 GYF domains.

Compound	Peptide sequence	Purity [%][c]	K_D [μM]
19a[a]	Ac-EFGPPPGWLGRFluo	96	111 ± 43
19b[a]	Ac-EFGPPPGWKGFluo	95	49 ± 15
19c[a]	Ac-EFGPPPGWKFluo	95	312 ± 106
19d[a]	Ac-EFGPPPGRKPFluo	98	385 ± 102
19e[a]	Ac-EFGPPPGRKFluo	95	460 ± 320
19f[a]	Ac-EFGPPPGFFluo	96	135 ± 31
19g[b]	Ac-FNGSPPGLGGGFluo	95	92 ± 32
19h[b]	Ac-FNGSPPGLERGFluo	99	168 ± 37
19i[b]	Ac-FNGSPPGLGGFluo	95	67 ± 21
19j[b]	Ac-FNGSPPGLGFluo	93	149 ± 26
19k[b]	Ac-FNGSPPGLFluo	92	188 ± 42
19l[b]	Ac-WRPGPPPPPPPPGLVFluo	97	441 ± 339
19m[b]	Ac-WRPGPPPPPPPGLFluo	96	80 ± 20

[a] For the CD2BP2 GYF domain. [b] For the PERQ2 GYF domain. [c] HPLC purity (220 nm) after purification

Table 4. Synthesized N-terminally fluorescein-labeled peptides for CD2BP2 and PERQ2 GYF domains.

Compound	Peptide sequence	Purity [%][c]	K_D [μM]
20a[a]	FluoEFGPPPGWLGR	99	12 ± 1.9
20b[a]	FluoEFGPPPGWLG	93	27 ± 7.5
20c[a]	FluoEFGPPPGWL	98	82 ± 19
20d[a]	FluoEFGPPPGW	99	183 ± 96
20e[a]	FluoEGPPPGWLGR	99	108 ± 24
20f[a]	FluoGPPPGWLGR	92	148 ± 33
20g[a]	FluoPPPGWLGR	92	132 ± 31
20h[a]	FluoPPGWLGR	95	295 ± 33
20i[a]	FluoEFGPPPGWKG	99	16 ± 2.7
20j[a]	FluoBpaEFGPPPGWLGR	99	2.3 ± 0.4
20k[a]	FluoEFGPPPGWLGRBpa	99	10 ± 7.0
20l[b]	FluoFNGSPPGLGG	95	285 ± 185
20m[b]	FluoPPGLSRD	96	177 ± 24
20n[b]	FluoSPPGLSRD	98	690 ± 218
20o[b]	FluoNGSPPGLSRD	95	994 ± 855
20p[b]	FluoWRPGPPPPPPPGLV	95	75 ± 16
20q[b]	FluoRPGPPPPPPPGLV	99	202 ± 38
20r[b]	FluoPGPPPPPPPGLV	98	338 ± 143
20s[b]	FluoWRPGPPPPPPPGL	95	46 ± 21

[a] For the CD2BP2 GYF domain. [b] For the PERQ2 GYF domain. [c] HPLC purity (220 nm) after purification.

and peptide solutions, the plate was shaken briefly, and polarization of the emitted fluorescence was directly recorded. FP values were plotted as a function of the logarithm of the protein concentration. Binding curves were fitted with the aid of GraphPad Prism software with a sigmoidal dose–response model (see the Experimental Section) and provided K_D values in the micromolar range (Table 3). For the CD2BP2 GYF domain, C-terminally labeled peptides with binding affinities around or below 100 μM were identified (**19a**, **19b**, **19f**), with **19b** being the highest-affinity ligand. To investigate the effect of the label position, the N-terminally labeled derivatives were also prepared and showed consistently higher affinity (namely **20a** and **20i**; 12 and 16 μM). The C-terminal (**20b**–**20d**) and

N-terminal (**20e**–**20h**) shortening of the sequence led to drastic declines in binding (Table 4), and so **20a** (Fluo-EFGPPPGWLGR-NH_2) was identified as the best fluorescence probe for the CD2BP2 GYF domain.

For the PERQ2 GYF domain, the C-terminally labeled probe **19i** (67 μM) was identified as the highest-affinity probe (Table 3). Again, to test the effect of the labeling position, the N-terminally labeled analogue **20l** was prepared and found to display significantly reduced affinity (285 μM, Table 4). For another test, a sequence containing seven consecutive prolines was investigated, and for this probe the N-terminally labeled peptide **20s** (46 μM) displayed a higher affinity than the C-terminally labeled analogue **19m**. In summary, it can be concluded that both C- and N-terminal labeling yields binding probes useful for FP measurements, and that the effect of the labeling position cannot be generalized and seems to depend on the specific peptide under investigation.

Evaluation of binding by NMR experiments

GYF domain binding of selected N-terminally fluorescein labeled peptides was confirmed by NMR spectroscopy. Increasing amounts of a fluorophore-modified peptide were added to ^{15}N-labeled GYF domain. HSQC NMR spectra were recorded and superposed to identify NH resonances of amino acid residues significantly shifted by ligand addition (Figure 4). Shifted amino acids were consistently located at the reported ligand binding site of this GYF domain.[7,30,31] For five fluorescein-labeled peptides the reversible binding affinities were determined by NMR titration (Table 5). Apparent K_D values were calculated by recording the chemical shifts of ten characteristic NH signals with increasing peptide concentration (Figure 5). All ten NH signals considered were located in proximity to the protein binding site as indicated in the three-dimensional protein structure (Figure 6). All peptides displayed slightly reduced binding affinities in the NMR titration experiments relative to fluorescence polarization. It should be noted that the NMR spectroscopy experiments record the binding to single NH positions, which can be reduced by the flexibility of the peptide

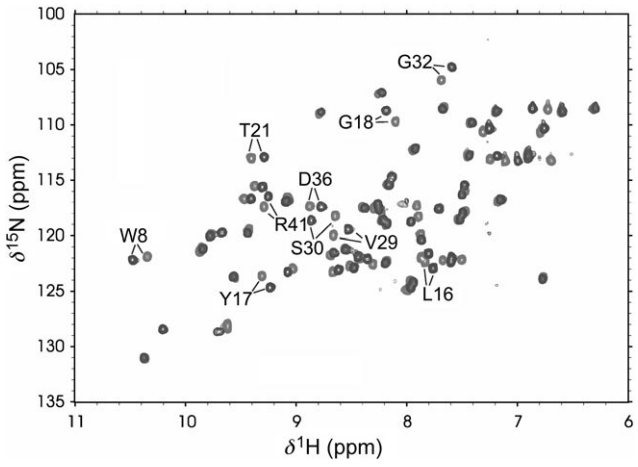

Figure 4. Overlays of the ^{15}N HSQC spectra for the CD2BP2 GYF domain without ligand (red) and upon addition of Fluo-EFGPPPGWLGR-NH_2 (**19l**, 2 mM, blue). Ten resonances showing the largest chemical shifts between the bound and unbound state used for K_D determination are labeled according to residue type and number.

Table 5. K_D values of N-terminally fluorescein-labeled peptides for CD2BP2 and PERQ2 GYF domains determined by NMR spectroscopy.

Compound	Peptide sequence	Purity [%][c]	K_D [μM]
20a[a]	FluoEFGPPPGWLGR	99	72 ± 8
20h[a]	FluoPPGWLGR	95	728 ± 118
20m[b]	FluoPPGLSRD	96	311 ± 52
20n[b]	FluoSPPGLSRD	98	487 ± 115
20p[b]	FluoWRPGPPPPPPPGLV	95	119 ± 11

[a] For the CD2BP2 GYF domain. [b] For the PERQ2 GYF domain. [c] HPLC purity (220 nm) after purification.

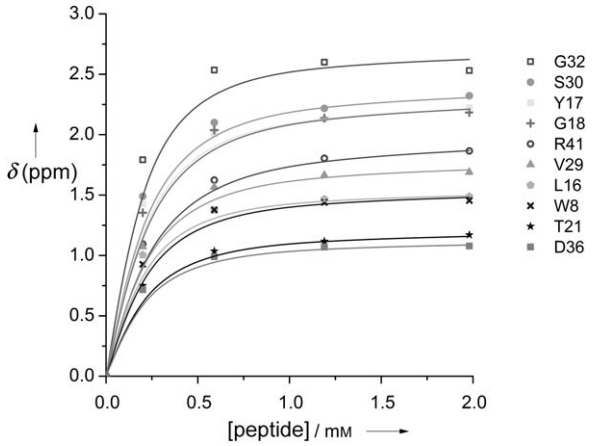

Figure 5. NMR titration of the CD2BP2 GYF domain with the peptide Fluo-EFGPPPGWLGR-NH_2 (**19l**). Large chemical shifts of ten resonances were plotted versus the peptide concentration. For curve fitting and K_D calculation with the Microcal™ Origin™ software, a simple two-state binding mode was assumed. Resulting K_D values were averaged.

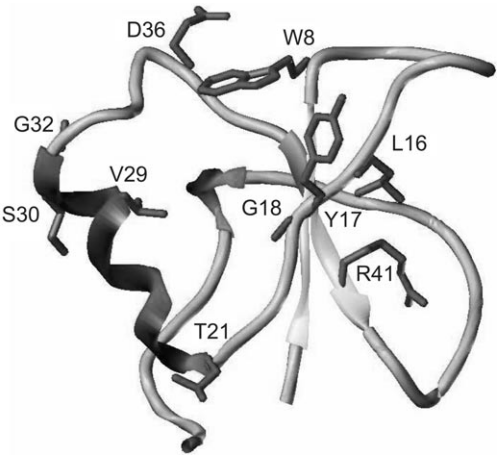

Figure 6. Ribbon structure of the CD2BP2 GYF domain (PDB ID: 1GYF), highlighting the secondary structure of the protein. Side chains of residues that were used as probes in the NMR titration experiments are shown in red and are labeled by amino acid type and sequence number.

ligand in the binding pocket. Moreover, the significantly higher DMSO concentrations in the NMR spectroscopy experiments can possibly account for overestimated K_D values, since it was found that DMSO can bind to the hydrophobic binding sites of GYF domains (C. Freund, unpublished observations). Relative affinities of different peptides, however, were identical for both methods (Tables 4 and 5).

Benzoylphenylalanine as affinity-enhancing element in competitive binding assays

Peptides with higher affinities towards the GYF domains were highly desirable to reduce the protein consumption of the assay. We reasoned that the use of photoactivated crosslinkers might increase the sensitivity of the assay considerably by turning the equilibrium binding assay into a kinetic photocrosslinking assay. Peptides **20j** and **20k**, with the photocrosslinker benzoylphenylalanine attached either C-terminally or N-terminally to the hitherto most active GYF binding peptide, were therefore synthesized. A significantly elevated K_D value of 2.3 μM was recorded for peptide **20k**. Irradiation of buffer solutions containing each of the pBPa peptides with an excess of CD2BP GYF at 350 nm led to no change in polarization even after 2 h. The observed affinity enhancement exerted by the benzoylphenylalanine thus cannot be attributed to photocrosslinking but is based on reversible ligand interaction. With peptide **20k** as a high-affinity probe, a competitive binding assay with unlabeled peptides as competitors and as positive controls was established. Reversible replacement of bound fluorescent probe was effected with high signal-to-noise ratio and reproducibility ($Z' = 0.79$). Accordingly, the developed assay should enable high-throughput screening of chemical libraries for GYF domain binding ligands.

Conclusions

A polymer support for the solid-phase synthesis of C-terminally labeled peptides has been developed. The polymer resin enables the direct attachment of peptides or other carboxylates to the amino functionality of aminofluorescein, thus offering direct and flexible access to fluorophore-labeled compound libraries. Fmoc-protected aminofluorescein was attached to 2-chlorotritylpolystyrene through a phenolic ether linkage, as verified by persistence of the lactone moiety as shown in the IR spectrum. MEM or silyl protecting groups were successfully used to protect free phenol hydroxyls. The suitability of this resin for producing C-terminally labeled peptides with photophysical properties useful for polarization measurements was demonstrated for two different proline-rich binding domains of the GYF family—CD2BP2 and PERQ2.

In a comparative study of C- and N-terminally labeled peptides, the effects of the labeling position on peptide binding were investigated. For this purpose, libraries of fluorescent peptides were prepared, and the binding to the two GYF protein domains was measured in fluorescence polarization experiments. Labels attached in both positions resulted in high-affinity ligands: in one of three examples, C-terminal labeling yielded peptides with significantly higher affinity than N-terminal fluorophore attachment, whereas in the other two cases N-terminal labeled peptides were superior. Site-directed binding of the peptide probes was verified by NMR titration experiments by recording of HSQC NMR spectra with ^{15}N-isotope-labeled proteins. For both domains, peptides with C- and N-terminally attached fluorophores were identified as GYF domain binders. Probes with K_D values smaller than 100 μM were identified for both domains under investigation, some of them possessing higher affinities than any other GYF domain ligand reported before. Introduction of the unnatural amino acid *p*-benzoylphenylalanine in one case yielded the first low-μM ligand for a GYF domain. With this peptide a competitive assay with high statistical reliability useable for screening of chemical libraries for GYF domain-interacting ligands was developed. It is intended to extend the introduction of affinity-enhancing amino acids to other signaling domains, such as SH3 and WW domains, in order to test the broader application of this concept for development of higher-affinity ligands.

The fluorescence labeling resin employed here for the preparation of fluorophore-labeled libraries of peptides should be applicable to the flexible and efficient preparation of fluorophore-labeled small-molecule libraries. Such libraries should create novel possibilities not only for binding assays, but also for the imaging of labeled molecules in cellular test systems.

Experimental Section

General methods: Unless otherwise noted, solvents and reagents were reagent grade from commercial suppliers and were used without further purification. Reactions were monitored by TLC on silica gel (60 F_{254}) plates with UV detection. LC-MS analyses were carried out on a C_{18} endcapped, 100 Å, 5 μM, 4×250 mm column (Macherey–Nagel, Nucleodur®) on an Agilent 1100 Series Liquid Chromatography Station equipped with a diode-array detector (DAD) and a Single Quadrupole Mass Spectrometer with electrospray ionization (ESI). The *m/z* range of 100–3000 was scanned in positive mode, with a voltage of 3000 V and a fragmentation of 70 V. The following gradient method was applied: eluent A (water + 0.1% formic acid), eluent B (acetonitrile + 0.1% formic acid), 5 to 100% B in 30 min, then 5 min isocratic 100% B, flow 0.8 mL min^{-1}. HPLC purity was determined at 254 ± 4 nm or 220 ± 4 nm. ^{1}H and ^{13}C NMR spectra were obtained on a Bruker AVANCE™ 300 MHz spectrometer and analyzed with Topspin 2.0.a. Peptide synthesis was conducted on a Multisyntech Syro multiple peptide synthesizer. UV/Vis absorption spectra were measured on a JASCO V-550 UV/Vis spectrophotometer. Fluorescence emission spectra were measured on a Cary Eclipse fluorescence spectrophotometer in a 1 cm quartz vessel. IR spectra were measured on a Nicolet Impact 400 series FT-IR spectrometer equipped with the PIKE MIRacle™ ATR-IR detection system.

Di-*O*-pivaloyl-4-aminofluorescein (2): Cs_2CO_3 (9.38 g, 28.8 mmol) was added to a solution of 4-aminofluorescein (**1**, 10.03 g, 28.8 mmol) in DMF (250 mL). The reaction mixture was cooled to 0 °C with an ice bath, and pivalic anhydride (13.37 mL, 72.0 mmol) was added dropwise. The solution was stirred for 2 h at room temperature. Cs_2CO_3 was filtered off, and DMF was evaporated in vacuo. The residue was diluted in ethyl acetate, washed with water and brine, dried with Na_2SO_4, filtered, and concentrated to yield **2** (14.61 g, 98%) as a yellow powder that was used as crude material

in the next step. ^{1}H NMR (300 MHz; CD_2Cl_2): δ = 1.36 (s, 18H; C*H*$_3$ *t*Bu), 6.80 (dd, J=8.6, 2.2 Hz, 2H; xanthene C*H*-2, 7), 6.90 (d, J=8.2 Hz, 1H; phenyl C*H*-6), 6.91 (d, J=8.5 Hz, 2H; xanthene C*H*-1, 8), 6.98 (dd, J=8.2, 2.0 Hz, 1H; phenyl C*H*-5), 7.06 (d, J=2.1 Hz, 2H; xanthene C*H*-4, 7), 7.18 ppm (d, J=1.9 Hz, 1H; phenyl C*H*-3); ^{13}C NMR (300 MHz; CD_2Cl_2): δ = 27.37 (CH_3, *tert*-Bu), 39.63 (C quat., *tert*-Bu), 82.03 (C quat., xanthene C-9), 108.71 (CH, phenyl C-3), 110.70 (CH, xanthene C-4, 5), 117.73 (C quat., xanthene C-8a, 9a), 118.22 (CH, xanthene C-2, 7), 123.00 (CH, phenyl C-5), 125.01 (CH, phenyl C-6), 128.26 (C quat., phenyl C-2), 129.51 (CH, xanthene C-1, 8), 142.64 (CH, phenyl C-1), 149.71 (CH, phenyl C-4), 152.28 (C quat., xanthene C-4a, 10a), 153.16 (C quat., xanthene C-3, 6), 169.98 (C quat., lactone C=O), 177.10 ppm (C quat., pivaloyl C=O); ESI-MS: *m/z* calcd: 515.19; found: 516.2 $[M+H]^+$; RP-HPLC t_r= 30.0 min, purity 92%.

Di-*O*-pivaloyl-4-(*N*-9-fluorenylmethoxycarbonyl)aminofluorescein (3): NaOH (1 N, 26.5 mL, 26.5 mmol) and Fmoc chloride (10.28 g, 39.7 mmol) were added stepwise at 0 °C over 1 h to a solution of **2** (14.61 g, 26.5 mmol) in THF (250 mL). The solution was stirred overnight at room temperature. THF was evaporated, water was added (250 mL), and the pH was adjusted to two with addition of $KHSO_4$. The product was extracted with ethyl acetate. The combined organic layers were washed with water and brine, dried with Na_2SO_4, filtered, and concentrated. The crude product was recrystallized from CH_2Cl_2/MeOH to yield white crystals of **3** (16.25 g, 85%). ^{1}H NMR (300 MHz; CD_2Cl_2): δ = 1.36 (s, 18H; C*H*$_3$ *tert*-Bu), 4.30 (t, J=6.3 Hz, 1H; Fmoc C*H*-9), 4.59 (d, J=6.3 Hz, 2H; Fmoc C*H*$_2$), 6.80 (d, J=8.6 Hz, 2H; xanthene C*H*-2, 7), 6.86 (d, J=8.6 Hz, 2H; xanthene C*H*-1, 8), 7.07 (s, 2H; xanthene C*H*-4, 5), 7.11 (d, J=8.3 Hz, 1H; phenyl C*H*-6), 7.33 (t, J=8.3 Hz, 2H; fluorenyl C*H*-2, 7), 7.42 (t, J=8.3 Hz, 2H; fluorenyl C*H*-3, 6), 7.66 (d, J=7.3 Hz, 2H; fluorenyl C*H*-1, 8), 7.68 (d, 1H; phenyl C*H*-5), 7.80 (d, J=7.4 Hz, 2H; fluorenyl C*H*-4,5), 8.10 ppm (s, 1H; phenyl C*H*-3); ^{1}H NMR (300 MHz; [D$_7$]DMF): δ = 1.36 (s, 18H; C*H*$_3$ *tert*-Bu), 4.41 (t, J=6.6 Hz, 1H; Fmoc C*H*-9), 4.60 (d, J=6.6 Hz, 2H; Fmoc C*H*$_2$), 7.04 (dd, J=8.6, 2.1 Hz, 2H; xanthene C*H*-2, 7), 7.10 (d, J=8.6 Hz, 2H; xanthene C*H*-1, 8), 7.31 (d, J=2.1 Hz, 2H; xanthene C*H*-4, 5), 7.40 (t, J=7.3 Hz, 2H; fluorenyl C*H*-2, 7), 7.44 (d, 1H; phenyl C*H*-6), 7.48 (t, J=7.3 Hz, 2H; fluorenyl C*H*-3, 6), 7.83 (d, J=7.8 Hz, 2H; fluorenyl C*H*-1, 8), 7.95 (d, 1H; phenyl C*H*-5), 7.98 (d, J=7.8 Hz, 2H; fluorenyl C*H*-4,5, 8.39 ppm (s, 1H; phenyl C*H*-3); ^{13}C NMR (300 MHz; CD_2Cl_2): δ = 27.38 (CH_3, *tert*-Bu), 39.66 (C quat., *tert*-Bu), 47.66 (CH, fluorenyl C-9), 67.65 (CH_2, Fmoc), 82.24 (C quat., xanthene C-9), 110.86 (CH, xanthene C-4, 5), 114.37 (CH, phenyl C-3), 116.95 (C quat., xanthene C-8a, 9a), 118.37 (CH, xanthene C-2, 7), 120.60 (CH, fluorenyl C-4, 5), 125.10 (CH, phenyl C-6), 125.52 (CH, fluorenyl C-1, 8), 126.45 (CH, phenyl C-5), 127.71 (CH, fluorenyl C-2, 7), 127.92 (C quat., phenyl C-2), 128.38 (CH, fluorenyl C-3, 6), 129.43 (CH, xanthene C-1, 8), 140.84 (C quat., phenyl C-1), 141.94 (C quat., fluorenyl C-4a, 4b), 144.30 (C quat., fluorenyl C-8a, 9a), 147.71 (C quat., phenyl C-4), 152.25 (C quat., xanthene C-4a, 10a), 153.35 (C quat., xanthene C-3, 6), 153.78 (C quat., Fmoc C=O), 169.24 (C quat., lactone C=O), 177.10 ppm (C quat., pivaloyl C=O); ^{13}C NMR (300 MHz; [D$_7$]DMF): δ = 26.73 (CH_3, *tert*-Bu), 39.16 (C quat., *tert*-Bu), 47.28 (CH, fluorenyl C-9), 66.81 (CH_2, Fmoc), 81.60 (C quat., xanthene C-9), 110.66 (CH, xanthene C-4, 5), 112.88 (CH, phenyl C-3), 117.15 (C quat., xanthene C-8a, 9a), 118.72 (CH, xanthene C-2, 7), 120.47 (CH, fluorenyl C-4, 5), 125.08 (CH, phenyl C-6), 125.53 (CH, fluorenyl C-1, 8), 126.07 (CH, phenyl C-5), 127.40 (C quat., phenyl C-2), 127.48 (CH, fluorenyl C-2, 7), 128.10 (CH, fluorenyl C-3, 6), 129.62 (CH, xanthene C-1, 8), 141.56 (C quat., fluorenyl C-4a, 4b), 142.12 (C quat., phenyl C-1), 144.40 (C quat., fluorenyl C-8a, 9a), 146.68 (C quat., phenyl C-4), 151.75 (C quat., xanthene C-4a, 10a), 153.17 (C quat., xanthene C-3, 6), 154.18 (C quat., Fmoc C=O), 168.91 (C quat., lactone C=O), 176.50 ppm (C quat., pivaloyl C=O); ESI-MS: *m/z* calcd: 737.26; found: 738.2 $[M+H]^+$; RP-HPLC r_t=33.7 min, purity >99%.

4-(9-Fluorenylmethoxycarbonyl)aminofluorescein (4)

*From compound **1***: NaOH (1 N, 2.88 mL, 2.88 mmol) and Fmoc chloride (1.12 g, 4.32 mmol) were added stepwise over 30 min at 0 °C to a solution of **1** (1.00 g, 2.88 mmol) in THF (10 mL). The solution was stirred for 3 h at room temperature. THF was evaporated, water was added (25 mL), and the pH was adjusted to 2 with addition of $KHSO_4$. The product was extracted with ethyl acetate. The combined organic layers were washed with water and brine, dried with Na_2SO_4, filtered, and concentrated. The crude product was purified with flash chromatography, first with hexane/ethyl acetate to elute the doubly protected by-product, and then the column was washed with dichloromethane/methanol to recover **4** (0.75 g, 46%, HPLC-purity 96%).

*From compound **3***: A solution of **3** (16.25 g, 22.1 mmol) in TFA (95%, 250 mL) was stirred overnight at 60 °C. TFA was evaporated, and the residue was dissolved in ethyl acetate and washed with water. The organic layer was extracted with aqueous Na_2CO_3 solution at pH 10 to transfer the product **4** into the aqueous layer, leaving unreacted traces of starting material **3** in the organic layer. The aqueous layer was washed with ethyl acetate, the pH was adjusted to pH 2–4 with addition of $KHSO_4$ salt, and extraction with ethyl acetate was carried out to transfer the product **4** back into the organic layer. The organic layer was washed with water and brine, dried with Na_2SO_4 and concentrated to yield **4** as an orange powder (11.54 g, 92%).

^{1}H NMR (300 MHz; [D$_7$]DMF): δ = 4.40 (t, J=6.9 Hz, 1H; Fmoc C*H*-9), 4.59 (d, J=7.0 Hz, 2H; Fmoc C*H*$_2$), 6.68 (dd, J=8.5, 2.0 Hz, 2H; xanthene C*H*-2, 7), 6.75 (d, J=8.5 Hz, 2H; xanthene C*H*-1, 8), 6.78 (d, J=1.9 Hz, 2H; xanthene C*H*-4, 5), 7.33 (d, J=8.4 Hz, 1H; phenyl C*H*-6), 7.40 (t, J=7.3 Hz, 2H; fluorenyl C*H*-2, 7), 7.48 (t, J=7.3 Hz, 2H; fluorenyl C*H*-3, 6), 7.83 (d, J=7.1 Hz, 2H; fluorenyl C*H*-1, 8), 7.93 (dd, 1H; J=8.4, 1.6 Hz, phenyl C*H*-5), 7.98 (d, J=7.8 Hz, 2H; fluorenyl C*H*-4,5), 8.32 ppm (d, J=1.4 Hz, 1H; phenyl C*H*-3); ^{13}C NMR (300 MHz; [D$_6$]DMSO): δ = 46.67 (CH, fluorenyl C-9), 65.75 (CH_2, Fmoc), 79.16 (C quat., xanthene C-9), 102.25 (CH, xanthene C-4, 5), 109.82 (C quat., xanthene C-8a, 9a), 112.51 (CH, phenyl C-3), 112.9 (CH, xanthene C-2, 7), 120.20 (CH, fluorenyl C-4, 5), 124.46 (CH, phenyl C-6), 125.08 (CH, fluorenyl C-1, 8), 125.67 (CH, phenyl C-5), 127.15 (C quat., phenyl C-2), 127.15 (CH, fluorenyl C-2, 7), 127.72 (CH, fluorenyl C-3, 6), 129.10 (CH, xanthene C-1, 8), 140.84 (C quat., phenyl C-1), 140.86 (C quat., fluorenyl C-4a, 4b), 143.68 (C quat., fluorenyl C-8a, 9a), 146.14 (C quat., phenyl C-4), 151.97 (C quat., xanthene C-4a, 10a), 153.54 (C quat., xanthene C-3, 6), 159.51 (C quat., Fmoc C=O), 168.64 ppm (C quat., lactone C=O); ESI-MS: *m/z* calcd: 569.15; found: 570.0 $[M+H]^+$; RP-HPLC r_t= 24.95 min, purity >99%.

4-(9-Fluorenylmethoxycarbonyl)aminofluorescein trityl resin (5): DIPEA (7.1 mL, 40.6 mmol) and 2-chlorotrityl chloride resin (11.2 g, 15.5 mmol, 1.4 mmol g^{-1}, 100–200 mesh, 1% DVB, Novabiochem®) were added to a solution of **4** (11.54 g, 20.3 mmol) in DCM/DMF (200 mL), and the reaction mixture was shaken for 3 h at room temperature. The solution was filtered off, and the resin was washed with DMF. The remaining free reactive sites were blocked by shaking the resin twice for 15 min in a MeOH/DMF mixture (1:9, *v/v*) with DIPEA (2.7 mL, 154.5 mmol). The resin was washed with DMF, THF, and DCM to furnish an orange resin 5 (0.26 mmol g^{-1}, 33%).

Di-*O*-(methoxyethoxymethyl)-4-(9-fluorenylmethoxycarbonyl)aminofluorescein trityl resin (6a): DIPEA (11.1 mL, 63.4 mmol) and MEM-Cl (6,24 mL, 52.8 mmol) were added to a suspension of **5** in DMF (200 mL). The reaction mixture was shaken for 90 min at room temperature. The resin was washed with DMF, THF, and DCM to yield **15a** (0.25 mmol g^{-1}, 100%) as a pale yellow resin.

Di-*O*-(*tert*-butyldimethylsilyl)-4-(9-fluorenylmethoxycarbonyl)aminofluorescein trityl resin (6b): The procedure was the same as for **15a**, with use of TBDMS-Cl.

Di-*O*-(triethylsilyl)-4-(9-fluorenylmethoxycarbonyl)aminofluorescein trityl resin (6c): The procedure was the same as for **15a**, with use of TES-Cl.

Di-*O*-(methoxyethoxymethyl)-4-aminofluorescein trityl resin (7): A suspension of **6a** in piperidine in DMF (20% 200 mL) was shaken for 2 min at room temperature, washed with DMF and shaken for another 10 min. The solution was filtered off, and the resin was washed with DMF, THF, and DCM to furnish **7** as an orange resin.

Solid-phase peptide synthesis: The coupling of the first amino acid was performed by adding Fmoc-protected amino acid (0.5 mmol) and DIC (77.6 μL, 0.5 mmol) to a suspension of **7** (100 mg, 0.05 mmol) in DCM/THF (1:1, *v/v*). The Fmoc group was removed by the procedure described above for compound **7** to yield **16**. The next amino acids were coupled by use of the Fmoc-protected amino acid (0.25 mmol), DIC (38.8 μL, 0.25 mmol), and HOBt (38.3 mg, 0.25 mmol) in DMF for 30 min, and the Fmoc group was removed. After each coupling, completion of the reaction was monitored with the Kaiser test, and the coupling was repeated if necessary. The last amino acid was then acetylated with acetic anhydride (0.2 mL) in DMF (1.4 mL) for 15 min to yield **18**. The completion of the reaction was monitored by the Kaiser test, and the acetylation was repeated if necessary. The peptide was cleaved off from the resin, and the fluorescein was deprotected by treatment with TFA in H_2O (95%) for 60 min, with addition of triisopropylsilane (2%), together with phenol (5%) for peptides containing Arg residues carrying a Pmc protecting group. The product **19** was precipitated by addition of the cleavage solution to cold diethyl ether (4 °C). After centrifugation (4000 min^{-1}, 5 min), the upper phase was removed from the vial, diethyl ether was added, the solid was washed for 5 min in an ultrasonic bath, and the vial was centrifuged. The procedure was repeated once more and the remaining solid was dissolved in *t*BuOH/H_2O (4:1, *v/v*) and lyophilized.

Fluorescence quantum yield determination: Solutions (10 μM) of fluorescein, 4-aminofluorescein, and peptides **20a** and **19l** in NaOH (aq., 0.1 M) were prepared. Absorption spectra were recorded to determine the ideal wavelength to be used for the fluorescence emission measurements: the wavelength at the intersection between the absorption curves of the sample and the standard, where both solutions have the same extinction coefficient, was chosen as excitation for the fluorescence measurement. The resulting emission curves were analyzed with Origin 7 software to determine their surfaces. Fluorescence quantum yields were calculated by use of the following equation: $\Phi = \Phi_{ref}\,(I/I_{ref})$, where Φ_{ref} is the quantum yield of the standard solution and I (or I_{ref}) is the fluorescence intensity of the sample (or the standard solution), given by the area under the emission curve.

Production of protein: The PERQ2 GYF and CD2BP2 GYF domains were expressed as GST fusion proteins in *E. coli* BL21 (DE3) cells harboring the plasmid pGEX 4T-1 with fragments either of PERQ2 (amino acids 531–596 of full-length PERQ2) or of CD2BP2 (amino acids 280–341 of full-length CD2BP2). *E. coli* cells were grown in lysogeny broth at 37 °C until an A_{600} of 0.5 was reached, and gene expression was induced with isopropyl-β-D-thiogalactopyranoside (IPTG; 1 mM). The culture was harvested after an additional 4 h of growth. GST fusion proteins were purified from the soluble fraction by affinity chromatography on a prepacked GSTrap™ HP glutathione-Sepharose column (GE Healthcare) and subsequent gel filtration (Superdex® 75, GE Healthcare) in phosphate-buffered saline (pH 7.3). Final protein concentrations were in the range of 0.2–0.4 mM in PBS.

Fluorescence polarization assays: The assays were carried out on 384-multiplates (low-volume, round-bottomed, black, nonbinding surface) from Corning (Nr. 3676) with 1×PBS (pH 7) as buffer in a final assay volume of 6 μL. The polarization measurements were performed on a GenioPro Reader from Tecan. The proteins were available as a solution of PERQ2 GYF domain (480 μM) and a solution of CD2BP2 GYF domain (480 μM) in 1×PBS buffer (pH 7.3). The synthesized peptides were first dissolved in DMSO and were then diluted with 1×PBS buffer (pH 7.3). The fluorescein-labeled peptide and the protein were placed on the plate and mixed briefly on an Eppendorf® MixMate™ shaker to give an assay composition of fluorescein-labeled peptide (10 nM) with various concentrations of protein in the presence of Tween (0.1%) and directly measured.

Fluorescence polarization measurements: The fluorescence polarization of the fluorescein-labeled molecules was determined by measuring the polarization with excitation at 485 nm and emission at 535 nm, with ten reads per well, an integration time of 40 μs and a gain of 90. Each measurement was repeated twice. The K_D values were determined by nonlinear curve fitting to a dose-response model with a variable slope with the aid of Prism software (Graph Pad Software, Inc., San Diego, CA).

Calculation of the *Z′* factor: The quality of a fluorescent probe for HTS was determined by calculating the *Z′* factor [Eq. (1)]:

$$Z' = 1 - \frac{3(\sigma_{bound} + \sigma_{free})}{mP_{bound} - mP_{free}} \quad (1)$$

where σ is the standard deviation and *mP* the fluorescence polarization value in *mP*. For the bound state, fluorescence polarization of Fluo-EFGPPPGWLGR-NH_2 (10 nM) was measured with GYF-CD2BP2 domain (12 μM) in PBS buffer (pH 7.3) and Tween (0.1%). To evaluate the free state, the unlabeled peptide EFGPPPGWLGR-NH_2 was added to a final concentration of 100 μM. A *Z′* value of 0.74 was determined. For the peptide Fluo-BpaEFGPPPGWLGR (**21j**) a *Z′* value of 0.79 was obtained at a protein concentration of 3.3 μM.

Protein NMR spectroscopy: The untagged ^{15}N-labeled GYF domain of human CD2BP2 was cloned and expressed as described elsewhere.[8] The His_6-tagged GYF domain of PERQ2 was cloned as described by Kofler et al.[29] The ^{15}N-labeled PERQ2 GYF domain was isolated from *Escherichia coli* BL21 (DE3) culture grown at 37 °C in M9 medium supplemented with $^{15}NH_4Cl$ until an A_{600} of 0.5 was reached. Gene expression was induced with IPTG (1 mM) for 4 h. Cells were disrupted by sonication, and the protein was purified from the soluble fraction by affinity chromatography on a prepacked HisTrap nickel-agarose column (GE Healthcare) and subsequent gel filtration. The NMR experiments were performed at 300 K on a Bruker DRX 600 instrument fitted with standard triple resonance probes. Data processing and analysis were carried out with the XWINNMR (Bruker) and SPARKY (SPARKY 3, version 3.1;

T. D. Goddard, D. G. Kneller, University of California at San Francisco) software packages.

In the NMR titration experiments, increasing amounts of synthesized peptides were added to samples (0.1 mM) of the ^{15}N-labeled CD2BP2 or PERQ2 GYF domain. Sample temperature was 300 K, and PBS with DMSO (5%) and D_2O (10%) was used as buffer. The gradual changes in chemical shifts of several isolated peaks in the heteronuclear single quantum coherence spectra were used for K_D calculation. The chemical shift changes for ^{15}N and ^{1}H atoms in a sample with peptide were determined as $((\Delta^1H)^2+(\Delta^{15}N)^2)^{1/2}$, where ^{1}H is in units of 0.1 ppm and ^{15}N is in units of 0.5 ppm. For curve fitting and K_D calculation with Microcal™ Origin™ software, chemical shift changes were plotted versus the peptide concentration, and a simple two-state binding mode was assumed.

Acknowledgement

C.F. and J.R. acknowledge the support of their work by the DFG (FOR806: "Interference with intracellular protein–protein interactions", Ra895/4) and the Leibniz Institute for Molecular Pharmacology (Integrating project 3: "Discovery of small molecule inhibitors of protein–protein interactions through fluorescence-based assays"). J.R. is grateful for continuous support of his work by the Fonds der Chemischen Industrie (FCI). We thank Dagmar Krause and Bernhard Schmikale for excellent technical support.

Keywords: fluorescence polarization · GYF domains · labeling · proline-rich sequences · protein–protein interactions

[1] T. W. J. Gadella, T. M. Jovin, R. M. Clegg, *Biophys. Chem.* **1993**, *48*, 221–239.
[2] P. B. Willoughby, G. Haughton, *J. Natl. Cancer Inst.* **1988**, *80*, 351–360.
[3] A. S. K. Dzik-Jurasz, *Br. J. Radiol.* **2003**, *76*, S98–109.
[4] P. R. Selvin, *Nat. Struct. Mol. Biol.* **2000**, *7*, 730–734.
[5] S. T. Hess, S. Huang, A. A. Heikal, W. W. Webb, *Biochemistry* **2002**, *41*, 697–705.
[6] G. Weber, *Biochem. J.* **1952**, *51*, 145–155.
[7] C. Freund, V. Dotsch, K. Nishizawa, E. L. Reinherz, G. Wagner, *Nat. Struct. Mol. Biol.* **1999**, *6*, 656–660.
[8] M. Kofler, K. Heuer, T. Zech, C. Freund, *J. Biol. Chem.* **2004**, *279*, 28292–28297.
[9] M. Kofler, K. Motzny, M. Beyermann, C. Freund, *J. Biol. Chem.* **2005**, *280*, 33397–33402.
[10] J. R. Lakowicz, *Principles of Fluorescence Spectroscopy*, Kluwer Academic/Plenum, New York, **1999**, pp. 291–320.
[11] The fluorescence lifetime (θ) is related to the molecular weight (M) in an approximation for globular molecules through the following equation: $\theta=\eta M(\nu+h)/(RT)$, where R is the ideal gas constant, T the absolute temperature, η the viscosity, ν the specific volume of the moiety, and h the hydration.
[12] R. Buchli, R. S. VanGundy, H. D. Hickman-Miller, C. F. Giberson, W. Bardet, W. H. Hildebrand, *Biochemistry* **2004**, *43*, 14852–14863.
[13] J. Schust, T. Berg, *Anal. Biochem.* **2004**, *330*, 114–118.
[14] R. Fischer, O. Mader, G. Jung, R. Brock, *Bioconjugate Chem.* **2003**, *14*, 653–660.
[15] P. J. A. Weber, J. E. Bader, G. Folkers, A. G. Beck-Sickinger, *Bioorg. Med. Chem. Lett.* **1998**, *8*, 597–600.
[16] J. R. Lakowicz, *Principles of Fluorescence Spectroscopy*, Kluwer Academic/Plenum, New York, **1999**, p. 69.
[17] C. R. Cantor, P. R. Schimmel, *Biophysical Chemistry, Part II: Techniques for the Study of Biological Structure and Function*, Freeman and Company, New York, **1980**, pp. 454–465.
[18] Perrin equation: $\frac{1}{p}-\frac{1}{3}=\left(\frac{1}{p_0}-\frac{1}{3}\right)\left(1+\frac{RT}{\eta V}\tau_0\right)$, where p is the polarization, p_0 the value of p when no depolarization takes place, R the ideal gas constant, T the absolute temperature, η the viscosity of the solvent, V the molecular volume of the fluorescent molecule, and τ_0 the fluorescence lifetime of the fluorophore.
[19] F. Zaragoza Dörwald, *Organic Synthesis on Solid Phase* Wiley-VCH, Weinheim, **2000**, pp. 1–11.
[20] W. Chan, *Fmoc Solid Phase Peptide Synthesis. A Practical Approach* (Eds.: W. C. Chan, P. D. White), Oxford University Press, **2000**.
[21] T. Hirano, K. Kikuchi, Y. Urano, T. Higuchi, T. Nagano, *J. Am. Chem. Soc.* **2000**, *122*, 12399–12400.
[22] V. Zanker, W. Peter, *Chem. Ber.* **1958**, *91*, 572–580.
[23] N. Klonis, W. H. Sawyer, *J. Fluoresc.* **1996**, *6*, 147–157.
[24] R. M. Silverstein, F. X. Webster, *Spectrometric Identification of Organic Compounds*, Wiley, **1997**, pp. 71–143.
[25] L. A. Carpino, D. Ionescu, A. El Faham, *J. Org. Chem.* **1996**, *61*, 2460–2465.
[26] J. L. Harris, B. J. Backes, F. Leonetti, S. Mahrus, J. A. Ellman, C. S. Craik, *Proc. Natl. Acad. Sci. USA* **2000**, *97*, 7754–7759.
[27] T. Imada, N. Cho, T. Imaeda, Y. Hayase, S. Sasaki, S. Kasai, M. Harada, H. Matsumoto, S. Endo, N. Suzuki, S. Furuya, *J. Med. Chem.* **2006**, *49*, 3809–3825.
[28] T. Mineno, T. Ueno, Y. Urano, H. Kojima, T. Nagano, *Org. Lett.* **2006**, *8*, 5963–5966.
[29] M. Kofler, K. Motzny, C. Freund, *Mol. Cell. Proteomics* **2005**, *4*, 1797–1811.
[30] M. Kofler, C. Freund, *FEBS J.* **2006**, *273*, 245–256.
[31] C. Freund, R. Kühne, H. Yang, S. Park, E. L. Reinherz, G. Wagner, *EMBO J.* **2002**, *21*, 5985–5995.

Received: May 14, 2008
Published online on September 18, 2008

